

Analysis of Cyclic Variations and Combustion Behavior of Liquid Phase Hydrocarbons Under Uniform Axial and Radial Magnetic Fields



Libin P. Oommen and G. N. Kumar

Abstract The present study experimentally investigates the combustion characteristics of a multi-cylinder MPFI spark ignition engine fuelled by gasoline under uniform magnetic fields. Permanent magnets made of N38 grade NdFeB are used to magnetize the liquid phase hydrocarbons and the impact produced on combustion characteristics like in-cylinder pressure and net heat release rate are studied under different speeds and load conditions of the engine operation. Three different magnetic intensities (3200 G, 4800 G, and 6400 G) are employed in two different magnetization patterns (axial and radial) at an inbuilt ignition timing of 5 deg bTDC. Magnetic field assisted combustion is observed to enhance the performance characteristics of the engine, while simultaneously reducing the exhaust emissions to a significant level. A statistical analysis of cyclic fluctuations in magnetic field-assisted combustion is also made which shows a reduction in fluctuations (COV) with the application of each stage of ionization. The increase observed in peak pressures and heat release rates along throughout the combustion cycles with reduction in cyclic variations indicate that magnetic field-assisted combustion exhibits better combustion characteristics as compared to normal gasoline combustion.

Keywords Combustion · Cyclic variation · Magnetic field · Peak pressure · Heat release rate · Coefficient of variation

L. P. Oommen (✉)

Department of Mechanical Engineering, Providence College of Engineering, Chengannur, India
e-mail: libinpanavelil@gmail.com

G. N. Kumar

Department of Mechanical Engineering, National Institute of Technology Karnataka, Surathkal, India

Nomenclature

COV	Coefficient of Variation
G	Gauss
IMEP	Indicated Mean Effective Pressure
NHRR	Net Heat Release rate
P	Pressure (N.m^{-2})

Greek Letters

θ	Crank angle location
μ	Mean of data population (Pa.s)
σ	Standard deviation of data population

Subscripts

Max	Maximum
-----	---------

1 Introduction

The accelerated depletion rate of conventional energy sources and the stringent regulations in exhaust emissions have made the researchers around the globe to focus on methods to enhance the combustion efficiency of the fuels. These methods include physical and chemical treatment of fuels, engine coatings, exhaust gas recirculation, catalytic reduction etc. Magnetic field-assisted combustion is an under-investigated technology of physical treatment of the fuel just before the injection into the cylinder.

Any hydrocarbon fuel is a molecule-by-molecule compound. These molecules are made up of atoms, which are made up of nuclei and electrons. These molecules form a cluster within themselves and will not actively interlock with oxygen molecules during combustion [1]. On the application of an external polarizing field, electrons are excited into states with a higher principal quantum number, resulting in the generation of a magnetic moment [2]. The induced magnetic moment alters the nuclear spin orientation and converts normal paramagnetic hydrogen molecules into the more reactive and unstable ortho state, resulting in the debilitating of Vandervaal's bonds and thus the de-clustering of the clusters formed due to intermolecular forces of attraction [2]. Subsequently, the penetration of oxidant to hydrocarbon structure is enhanced which will result in the active interlocking between fuel and oxygen molecules, ensuring complete combustion [3].

In the thermodynamic perception, fuel consumption of an engine is directly dependent on the values of combustion enthalpy. This combustion enthalpy is quantified using the bonding energy of reactants and products [4]. The polarizing field is found to alter the bonding energies of fuel molecules, thereby effecting the combustion enthalpies and subsequently reducing the consumption of fuel [5]. The applicability of magnetic polarization in increasing the energy efficiency of fishing vessels was examined by Gabina et al. [6]. Their experiments on three compression ignition engines yielded that the fuel consumption was found to decline at higher loads in-situ conditions. The impact of magnetic fields on hydrocarbon-based R600 refrigerant and non-hydrocarbon-based R134A for a vapor compression system was experimentally analyzed by Khedawan and Gaikwad [7]. Fuel economy improved and exhaust concentration decremented for hydrocarbon-based refrigerant upon polarization [8].

Gad [9, 10] experimentally studied the impact of exposure of polarizing magnetic fields on a single cylinder, four-stroke Kirloskar CI engine at full load and no load conditions. The fuel economy improved by 3 to 8.5% from no load till full load conditions. The emission of Carbon monoxide showed a reduction of 10% and 4.5% whereas oxides of nitrogen declined by 13% and 24% respectively. The influence on the combustion and emissions of a generator fuelled by diesel when a magnetic tube is incorporated in the fuel intake was examined by Chen et al. [11]. Kurji and Imran [12] installed permanent magnetic assembly before the injection pump in a single cylinder four stroke CI engine and observed a reduction of 15.71% in the consumption of fuel induced due to reduced surface tension due to applied fields.

The operating parameters of spark ignition engines are limited by cyclic variations. The flame propagation in SI engines is dependent on condition of the mixture and airflow in the region of sparking at the time of spark which directly influences cyclic variations. Aydin [13] concluded that average laminar flame velocity, intensity of turbulence, and velocity are the elements that influence cyclic fluctuations in combustion. Ceviz et al. [14] studied the impact of AFR on cyclic variations in a lean combustion system. Their results prove that an increase in air-fuel ratio will result in increased cyclic variations. Studies have proven that a surge in power harvest for the same amount of fuel consumed can reduce cyclic variations in combustion [15, 16]. From early days, combustion in an engine is studied in terms of cylinder pressure. The magnitude (P_{max}) and location of maximum pressure (θ_{pmax}) are the most commonly utilized parameters for analyzing combustion. The major downfall in the case of parameters derived directly from pressure is the insufficient knowledge of on-going cylinder processes [17]. Coefficient of Variation of IMEP is an effective parameter that indicates engine behavior because it visualizes the torque fluctuations [18]. Experimental studies on the combustion and emission characteristics of an MPFI engine fuelled by liquid phase and gas phase fuels proved that magnetic polarization is beneficial in enhancing the performance characteristics [19–23]

2 Description of Experimental Rig and Instrumentation

The experimental setup and instrumentation consists of a multi-cylinder four stroke engine of Maruthi Zen as depicted in Fig. 1. The required load to the engine is applied by an eddy current dynamometer and imperative instruments for sensing combustion pressures and corresponding crank angles are provided. The signals obtained from these instruments are interfaced to the PC using NI-based USB-6210 data acquisition system. IC Engine Soft V 15.0, commercially available combustion analysis software, is employed for online combustion evaluation.

High-grade NdFeB magnets are installed on the fuel line using special fixtures to produce the required magnetization pattern. The losses in magnetic intensity during the operation are prevented through the administration of a stainless steel covering to the magnetic assembly. The cyclic variations in combustion are studied under axial and radial patterns of magnetization.

The magnetic intensity of permanent magnets is measured using a gauss meter which is named after the great scientist Carl Friederich Gauss. The modern Gauss meter is an advanced version of Gauss' magnometer. It consists of a gauss probe, the meter, and a cable for connection and works on the principle of Hall effect. To measure the magnetic intensity, the instrument is switched on and the probe which is available on the end is placed on the magnet to be measured. When the magnet is slid over the sensor, the highest rating picked up on the meter is noted which corresponds to the Gauss value of that particular magnet. Both the intensity and direction of magnetic fields can be measured using this instrument.

The instruments are calibrated before they are used in the experimental data collection. The dynamometer, load cell, exhaust gas analyzer, and the pressure transducer are calibrated by their respective suppliers. The repeatability of data is ensured when the experiment is conducted. Prior to the data acquisition, the engine is operated for some time to reach steady state operation. Experimental error is minimized by taking average value of three readings at each test points. Periodic leak checks are done for LPG fuel line and injectors to ensure safety. Fire extinguishers are provided near to

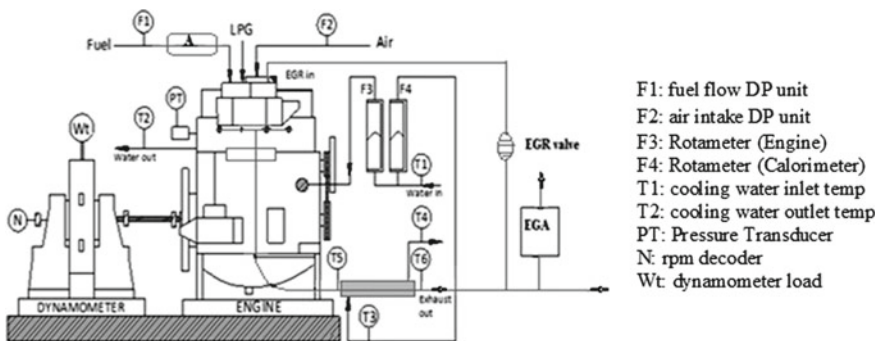


Fig. 1 Schematic representation of engine test rig and associated parts

the rig in case of any occurrence of fire. Storage devices like HDD are kept away at a safe distance from the strong magnetic field. A warning board is also hung to keep away people with pacemakers from the impact of magnetic fields.

3 Analysis of Combustion Parameters and Combustion Stability

The heat release analysis is effectuated on the basis of first law of thermodynamics with the intake and exhaust valves closed making the engine a closed system. The cylinder contents are considered to be a single zone of which the thermodynamic properties are uniform and constituted by mean values. The first law of thermodynamics as applicable to this case can be expressed as

$$\frac{dQ}{dt} - p \frac{dV}{dt} + \sum_i m_i h_i = \frac{dU}{dt}$$

where Q is the heat transferred (J), p is the pressure (Pa), V is the volume (cubic meter), m_i is the mass of injected fuel, h_i is the enthalpy (J/kg), and U is the internal energy (J). The only mass which is crossing the system boundary is the injected fuel and hence the mass-enthalpy term in the expression can be reframed to mass of fuel enthalpy. Using a simplified assumption that the net heat release is the difference in energy released from combustion and the energy lost to the walls through heat transfer, the above equation can be reframed to

$$\frac{dQ}{dt} = p \frac{dV}{dt} + \frac{dU}{dt}$$

If a further assumption can be made that the contents of the cylinder can be modeled as ideal gas

$$\frac{dQ}{dt} = p \frac{dV}{dt} + mc_v \frac{dT}{dt}$$

In which c_v corresponds to the specific heat at constant volume. The temperature term in this expression can be eliminated by differentiating the ideal gas law because temperature term is mostly unavailable in pressure analysis.

$$\frac{dQ_{\text{net}}}{dt} = \frac{\gamma}{\gamma - 1} p \frac{dV}{dt} + \frac{1}{\gamma - 1} V \frac{dp}{dt}$$

In this equation, γ corresponds to the ratio of specific heats and Q_{net} is the net heat release rate in J/deg. In a spark ignition engine the value of γ is obtained by matching single zone model analysis to a two zone model analysis for various fuels.

Heat transfer in the combustion chamber occurs by both convection and radiation in between the burning gases, cylinder walls, cylinder head, intake, and exhaust valves and piston during the working cycle. Among the two modes, convection comprises the major part. Considering the impact of heat transfer to the walls of combustion chamber, the gross heat release is expressed as

$$\frac{dQ_{\text{Gross}}}{d\theta} = \frac{dQ_{\text{Net}}}{d\theta} + \frac{dQ_{\text{ht}}}{d\theta}$$

4 Results and Discussion

The combustion characteristics of an engine are best represented using in-cylinder pressure variation and net heat release rate with respect to the crank angle locations. Here, the cyclic variations in combustion are analyzed at four different speeds of the engine (3500 rpm, 3000 rpm, 2500 rpm, and 2000 rpm) and full load condition. Figures 2, 3, 4, and 5 show the average cylinder pressures in 100 consecutive cycles at four engine speeds and four stages of axial magnetization (no magnetization, 3200 G, 4800 G, and 6400 G).

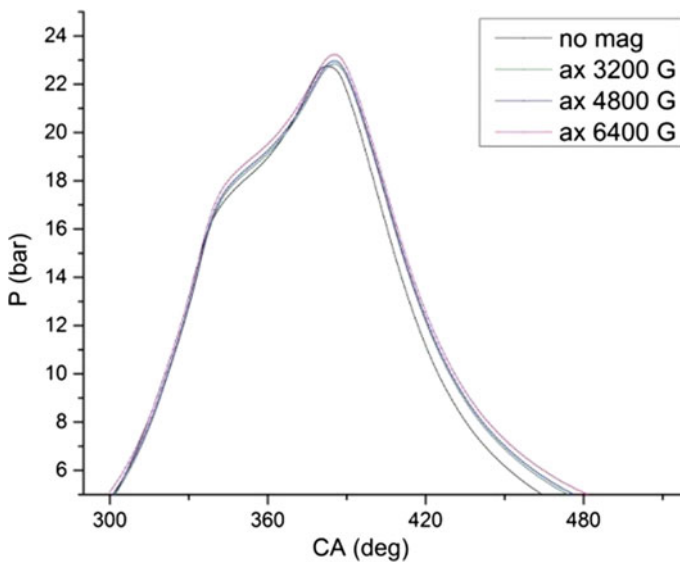


Fig. 2 In-cylinder pressure at 3500 rpm

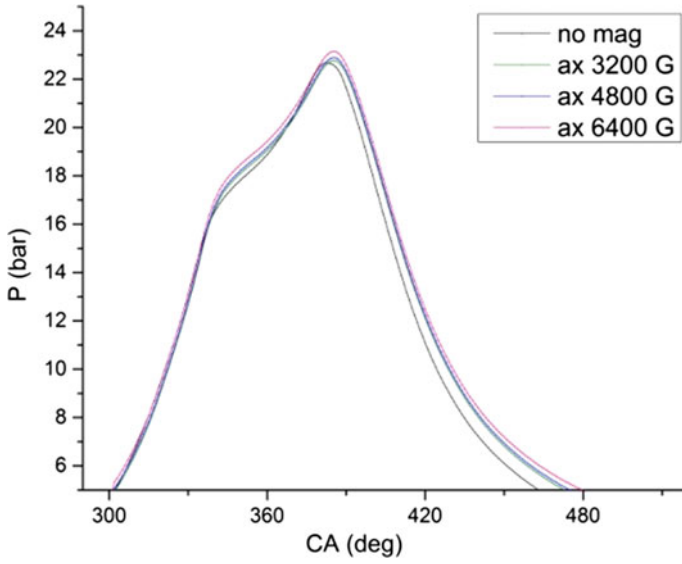


Fig. 3 In-cylinder pressure at 3000 rpm

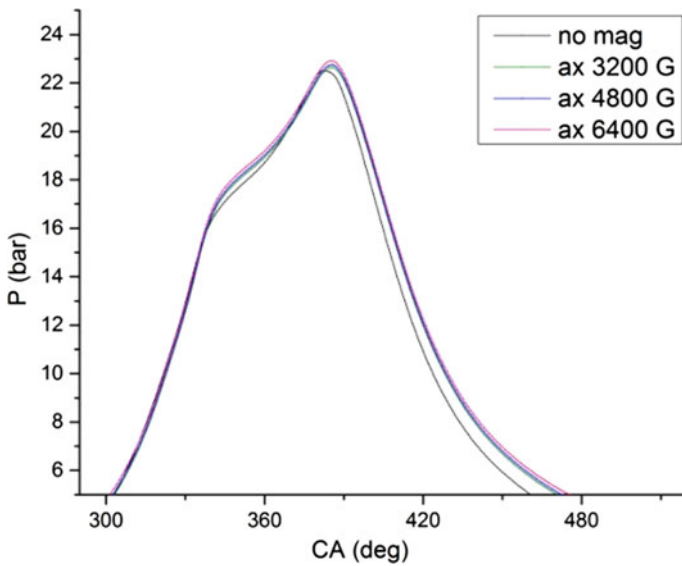


Fig. 4 In-cylinder pressure at 2500 rpm

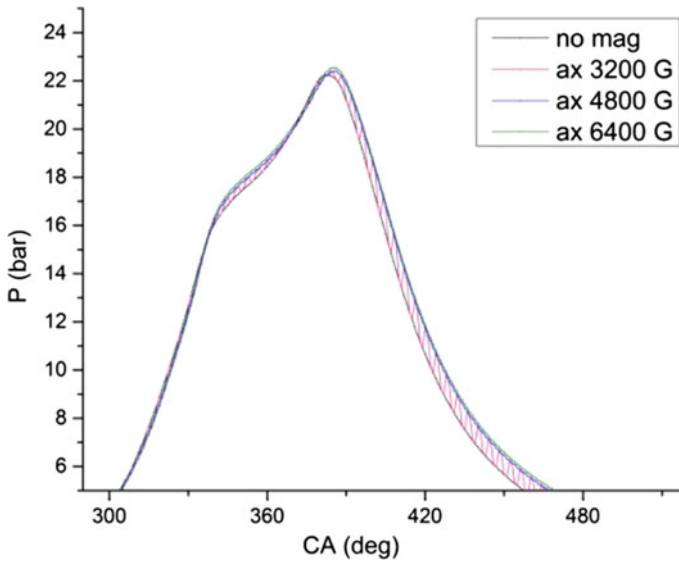


Fig. 5 In-cylinder pressure at 2000 rpm

4.1 Combustion Characteristics Under Axial Magnetization Pattern

It can be observed that there is a small variation in pressures between the magnetized and non-magnetized conditions even though the engine is operated under the same fuel and at the same speed. The peak pressure is found to increase with each stage of magnetization and is maximum at 6400 G for all the speeds. The highest value of cylinder pressure observed (P_{\max}) is 23.23 bar at 3500 rpm and at 6400 G magnetic intensity, which is 2.75% higher than the case of same engine speed without magnetization. The increase in peak pressure indicates the enhancement of combustion properties with higher intensities of magnetization.

The stability of combustion is one of the most important parameters to be analyzed whenever a modification in fuel or operating parameters is experimented on an engine. The extent of lean burning and tolerance of EGR are all subjected to the stability of combustion. Although the stability of combustion could be deduced from the engine performance and emission data, a substantial and conclusive evidence of it can be made through a statistical analysis of coefficient of variation (COV) of indicated mean effective pressures and peak pressures during the working cycle (Figs. 6 and 7).

The NHRR characteristics for experimented speeds of the engine at full load operation and all the tested intensities of axial fields are shown in Figs. 8, 9, 10, and 11. The net heat release rate is an effective means to analyze the combustion phenomena critically. This parameter has the advantage of identifying combustion

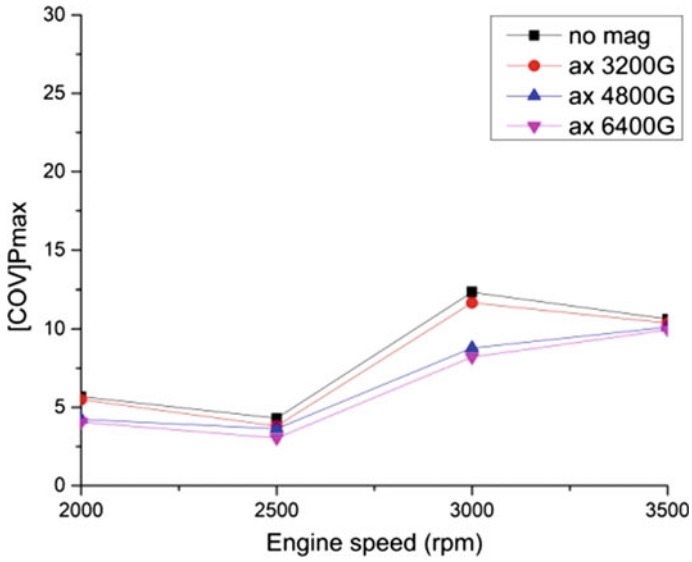


Fig. 6 COV of P_{max} in axial magnetization

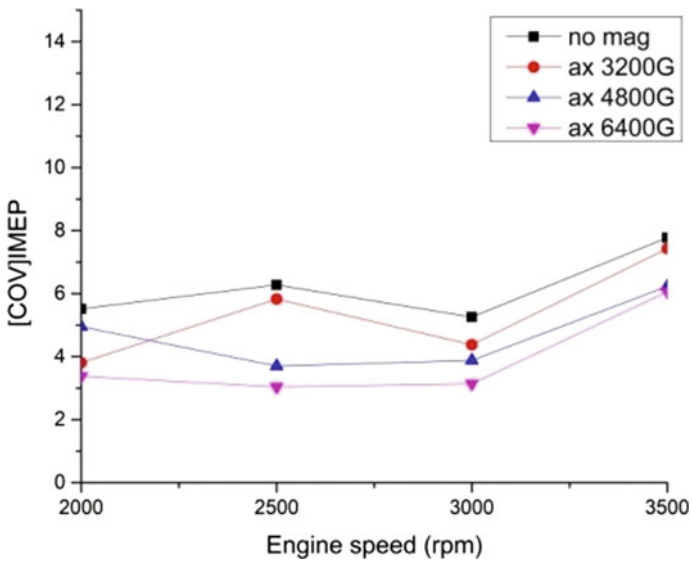


Fig. 7 COV of IMEP in axial magnetization

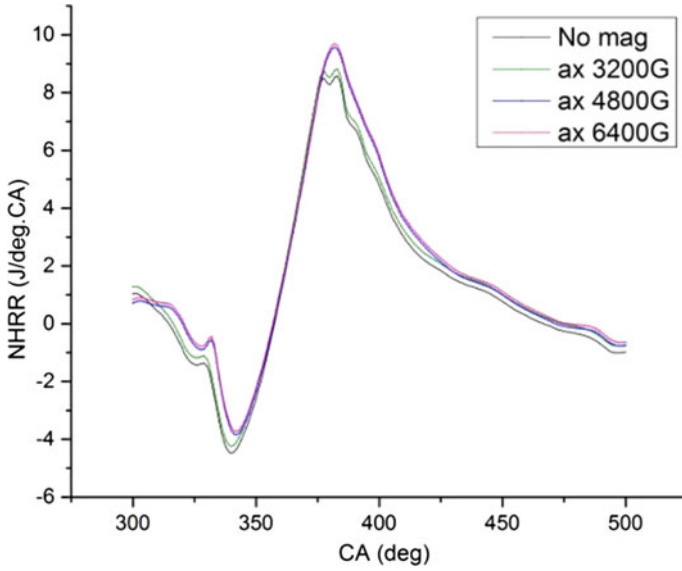


Fig. 8 NHRR at 3500 rpm in axial magnetization

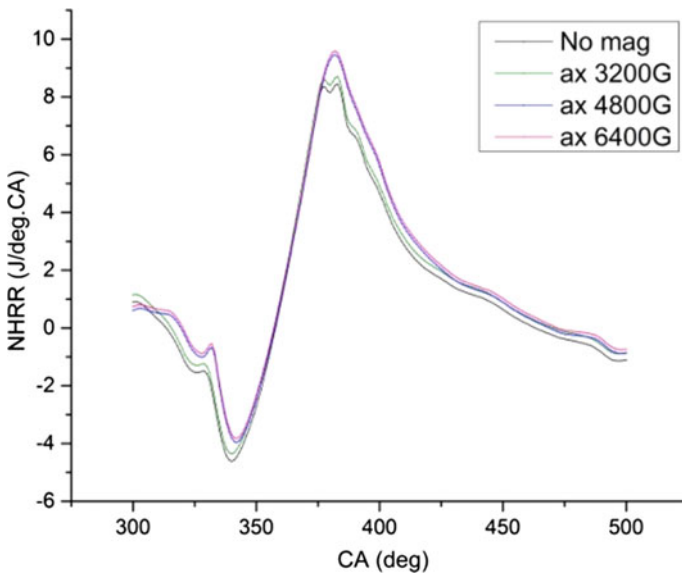


Fig. 9 NHRR at 3000 rpm in axial magnetization

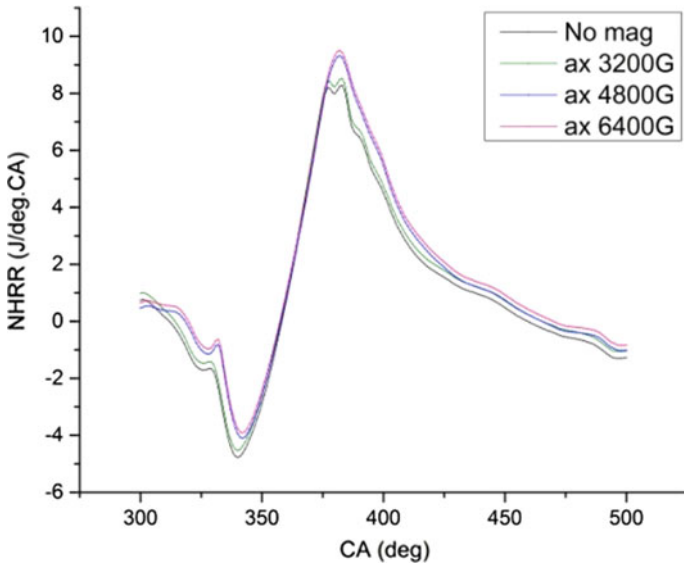


Fig. 10 NHRR at 2500 rpm in axial magnetization

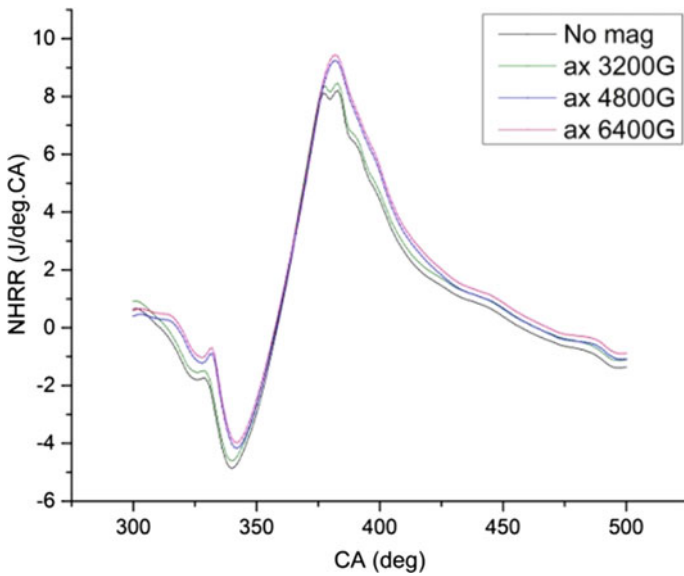


Fig. 11 NHRR at 2000 rpm in axial magnetization

indicators like ignition delay, duration of combustion, rate of heat release, and its crank angle locations.

As seen in the figures, the rate of heat release increases with increasing intensity of magnetization. Though the duration of heat release has not varied, the locations of maximum heat release vary with higher intensity of magnetization. This may be due to the fact that hydrocarbons have realigned themselves on subjected to magnetic fields, breaking the normally occurring clustered structure, thus making the combustion more efficient.

4.2 Combustion Characteristics Under Radial Magnetization Pattern

In the second stage of experimentation, the cyclic variations in combustion are analyzed under radial magnetization pattern. The engine is operated under the same load and speed conditions as in the case of axial magnetization. Figures 12, 13, 14, and 15 represent the variation in in-cylinder pressures in 100 consecutive cycles under four stages of radial magnetization.

As observed in the case of axial magnetization, the cylinder pressure increased with the increase in intensity of applied magnetic field and is maximum in the case of 6400 G. The highest magnitude of cylinder pressure observed (P_{\max}) is 23.91 bars at 3500 rpm and at 6400 G magnetic intensity, which is 4.89% higher than the case

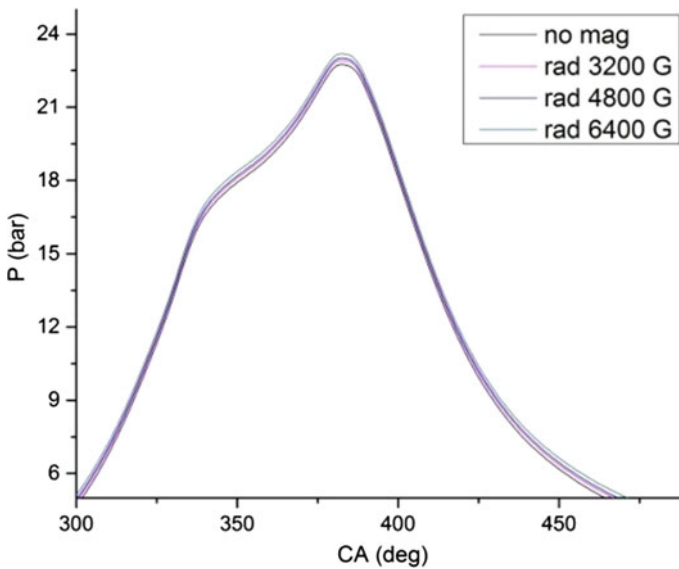


Fig. 12 In-cylinder pressures at 3500 rpm in radial magnetization

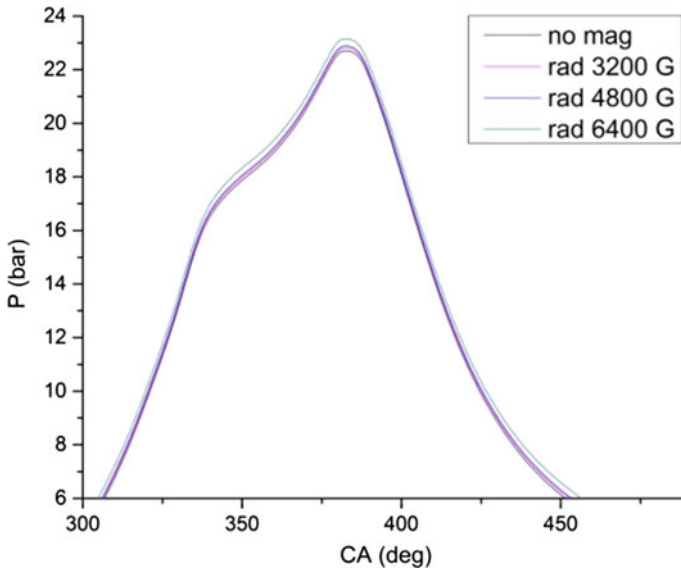


Fig. 13 In-cylinder pressures at 3000 rpm in radial magnetization

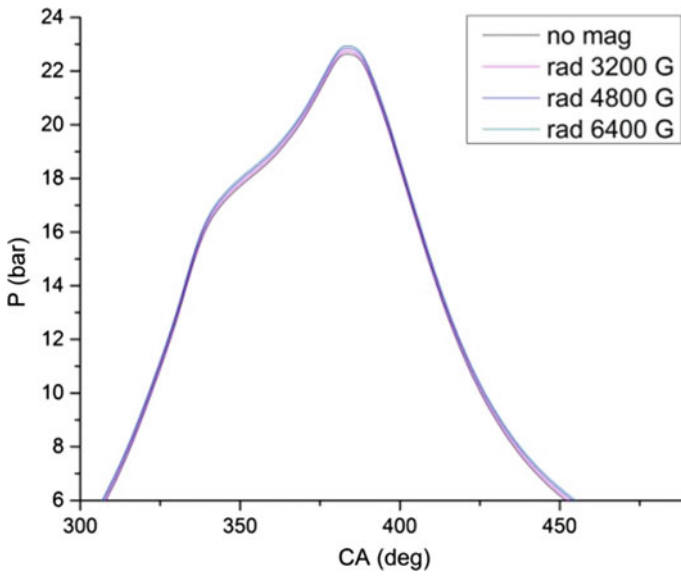


Fig. 14 In-cylinder pressures at 2500 rpm in radial magnetization

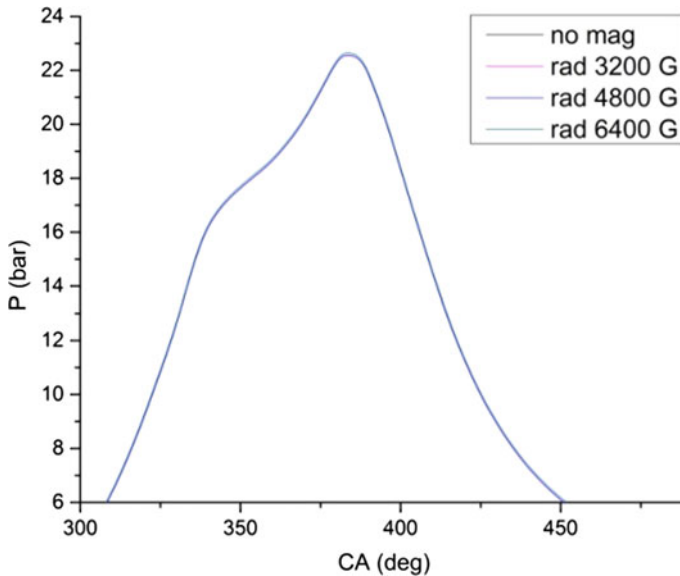


Fig. 15 In-cylinder pressures at 2000 rpm in radial magnetization

of same engine speed without magnetization. When both the magnetization patterns are compared, the peak pressure in the case of radial magnetization is 2.14% higher than that in the case of axial magnetization. This may be due to the fact that the radial magnetization pattern is shown to produce more underling torque and torque ripple than an axial field of similar intensity [24] (Figs. 16 and 17).

The statistical investigation of fluctuations of P_{\max} and IMEP throughout the combustion cycles shows analogous results as in the case of axial magnetization. The damping of fluctuations in maximum pressure and mean effective pressures is due to the enhancement in combustion and yielding of more output power for the same amount of fuel burnt.

The analysis of NHRR also provides similar information on combustion character in radial pattern. The peak location of heat release regularly increased with each stage of magnetization and is maximum in the case of 6400 G. This increase in combustion efficiency due to magnetization reflects in the operational characteristics and thermal efficiency of the engine as well. The NHRR characteristics under radial magnetization are shown in Figs. 18, 19, 20, and 21.

The heat release pattern and the duration of heat release are found to be similar in both cases of magnetization. The higher rate of heat release may also be attributed to the increased penetration of oxygen molecules into the interior carbon atoms in the hydrocarbon chain [20, 25]. However, the ability of radial magnetization to decluster and re-align the hydrocarbon molecules is higher when compared to axial pattern and this results in efficient combustion.

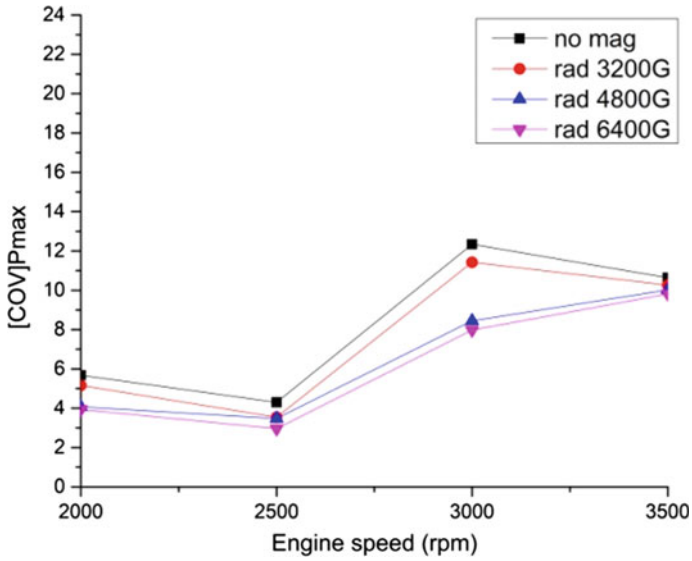


Fig. 16 COV of P_{max} in radial magnetization

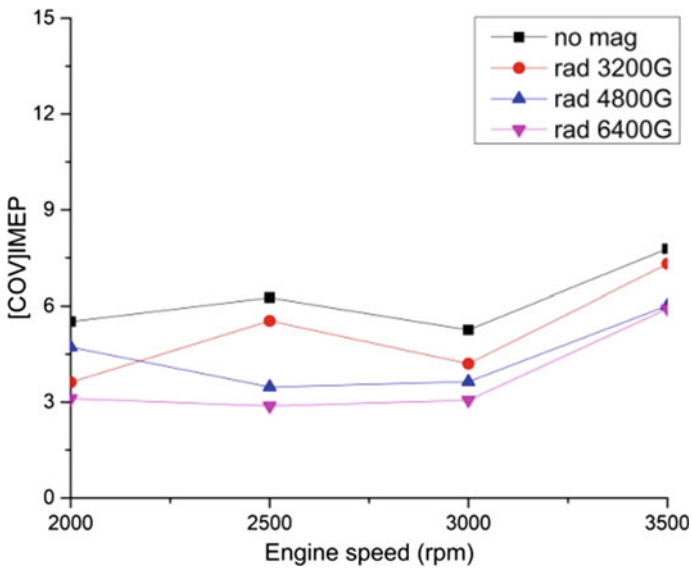


Fig. 17 COV of IMEP in radial magnetization

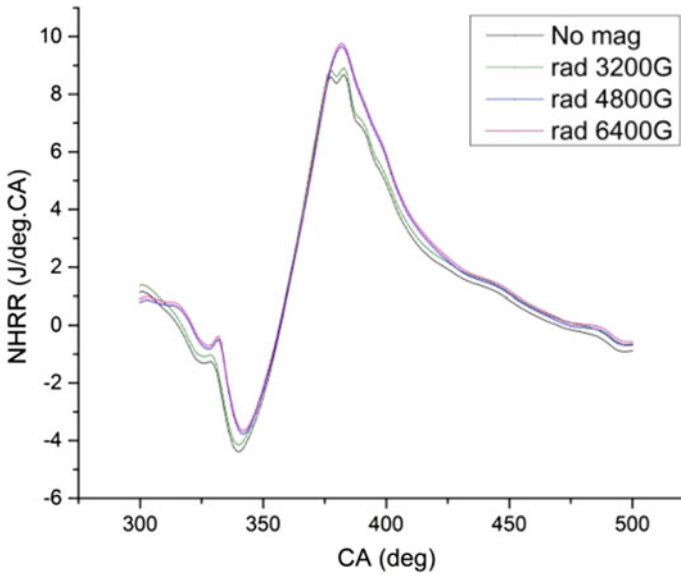


Fig. 18 NHRR at 3500 rpm in radial magnetization

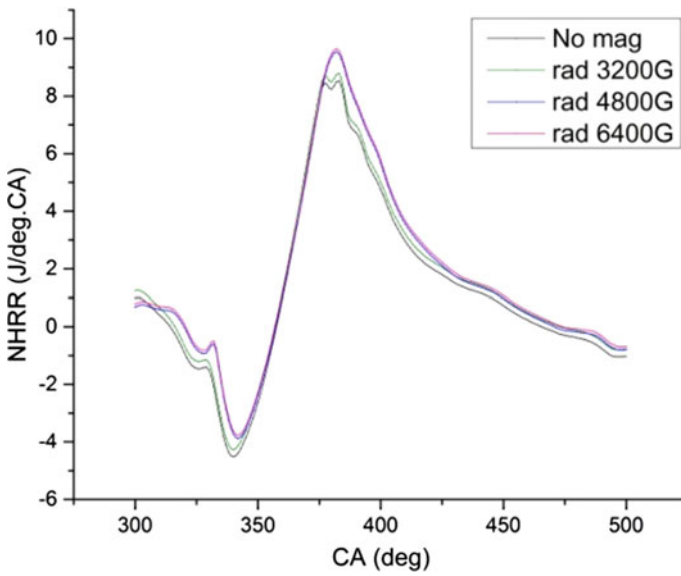


Fig. 19 NHRR at 3000 rpm in radial magnetization

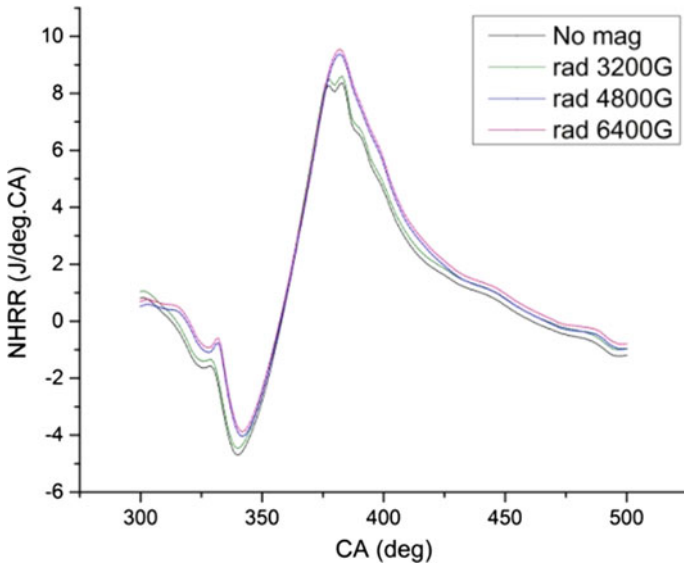


Fig. 20 NHRR at 2500 rpm in radial magnetization

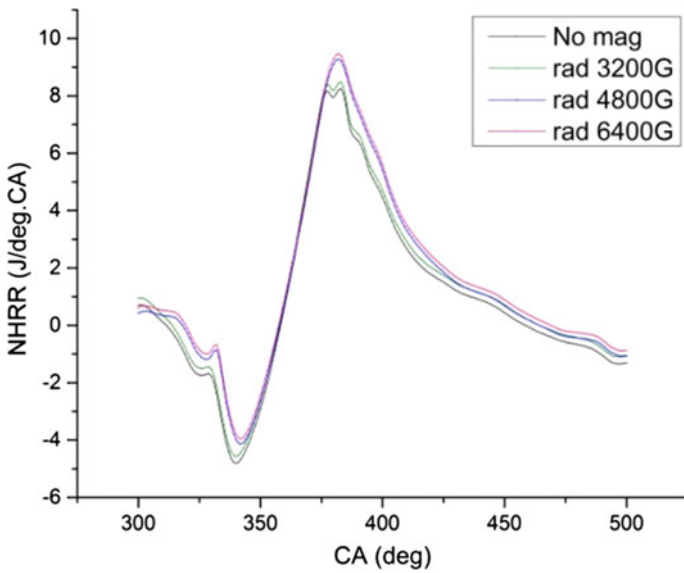


Fig. 21 NHRR at 2000 rpm in radial magnetization

5 Conclusions

An experimental study was conducted on a multi-cylinder MPFI engine to analyze the combustion characteristics of gasoline under four stages of intensities and two patterns of magnetization. The major findings of the experimental study can be summarized as:

- Increase in intensity of magnetization results in higher in-cylinder pressures and P_{\max} values in both patterns of magnetization.
- The rate of heat release increased with increased strength of the applied magnetic field. However, the heat release pattern and the duration of combustion remained similar.
- Radial magnetization pattern is found to increase the peak pressure value by 4.89% whereas axial magnetization is found to enhance the same by 2.75%. The net heat release rate under radial magnetization is also found to be higher than that of axial magnetization.
- The statistical investigation of fluctuations of P_{\max} and IMEP throughout the combustion cycles shows that the fluctuations and cyclic variations in combustion reduce with increase in intensity of the applied magnetic field and also with a change in magnetization pattern to radial fields.

Acknowledgements This work was supported by the Internal Combustion Engines research laboratory and fuels laboratory of NITK Surathkal. The necessary instrumentation was provided by Unisource Industrials, Bengaluru, and Rex Associates Mangaluru. These supports are gratefully acknowledged.

References

1. Faris AS et al (2012) Effects of magnetic field on fuel consumption and exhaust emissions in two-stroke engine. *Energy Procedia* 18:327–338
2. Fatih FA El, Gad M (2010) Effect of fuel magnetism on engine performance and emissions. *Aust J Basic Appl Sci* 4:6354–8
3. Kumar PV et al (2014) Experimental study of a novel magnetic fuel ionization method in four stroke diesel engines. *Int J Mech Eng Rob Res* 3:151–159
4. Oommen LP, Kumar GN (2019) A study on the effect of magnetic field on the properties and combustion of hydrocarbon fuels. *Int J Mech Prod Eng Res Dev* 9:89–98
5. Govindasamy P, Dhandapani S (2007) Performance and emissions achievements by magnetic energizer with a single cylinder two stroke catalytic coated spark ignition engine. *J Sci Ind Res* 66:457–463
6. Gabiña G et al (2015) Energy efficiency in fishing: are magnetic devices useful for use in fishing vessels ? *Appl Therm Eng* 94:670–678
7. Khedvan AVG (2015) Review on effect of magnetic field on hydrocarbon refrigerant in vapor compression cycle. *Int J Sci Eng Technol* 4:1374–8
8. Patil S, et al (2017) Effect of magnetic field on hydrocarbon refrigerant, pp 1443–9
9. Gad MS et al (2016) Effect of fuel magnetism on industrial oil burner performance burning waste cooking oil. *Int J Eng Technol* 16:25–37

10. El-Baz FK et al (2017) Comparative study of performance and exhaust emissions of a diesel engine fueled with algal, used cooked and Jatropha oils biodiesel mixtures. *Int J Mech Mechatron Eng* 17:90–100
11. Chen CY et al (2017) Impact of magnetic tube on pollutant emissions from the diesel engine. *Aerosol Air Qual Res* 17:1097–1104
12. Kurji HJ, Imran MS (2018) Magnetic field effect on compression ignition engine performance. *ARN J Eng Appl Sci* 13:3943–3949
13. Aydin K (2011) Effect of engine parameters on cyclic variations in spark ignition engines, proceedings of 6th international advanced technology symposium, vol 16. Elazığ, Turkey, pp 57–63
14. Ceviz MA et al (2011) Analysis of the thermal efficiency and cyclic variations in a SI engine under lean combustion conditions. *J Therm Sci Technol* 31:121–127
15. Litak G et al (2007) Cycle-to-cycle oscillations of heat release in a spark ignition engine. *Meccanica* 42:423–433
16. Litak G et al (2009) Combustion process in a spark ignition engine: Analysis of cyclic peak pressure and peak pressure angle oscillations. *Meccanica* 44:1–11
17. Johansson B (1996) Cycle to cycle variations in SI engines—the effects of fluid flow and gas composition in the vicinity of the spark plug on early combustion, SAE technical paper. <https://doi.org/10.4271/962084>
18. Nayak V et al (2015) Combustion characteristics and cyclic variation of a LPG fuelled MPFI four cylinder gasoline engine. *Energy Procedia* 90:470–480
19. Oommen LP, Kumar GN. Influence of magneto combustion on regulated emissions of an automotive engine under variable speed operation. *Int J Veh Struct Syst* 11. <https://doi.org/10.4273/ijvss.12.1.25>
20. Oommen LP, Kumar GN (2020) Experimental studies on the impact of part-cooled high-pressure loop EGR on the combustion and emission characteristics of liquefied petroleum gas. *J Therm Anal Calorim* 141:2265–2275. <https://doi.org/10.1007/s10973-020-09762-0>
21. Oommen LP, Kumar GN (2020) Experimental studies on the influence of axial and radial fields of sintered neo-delta magnets in reforming the energy utilization combustion and emission properties of a hydrocarbon fuel. *Energy sources, part A: recovery, utilization, and environmental effects*. <https://doi.org/10.1080/15567036.2020.1767729>
22. Oommen LP, Narayanappa KG, Vijayalakshmi SK (2020) Experimental analysis of synergetic effect of part-cooled exhaust gas recirculation on magnetic field-assisted combustion of liquefied petroleum gas. *Arab J Sci Eng* 45:9187–9196. <https://doi.org/10.1007/s13369-020-04696-z>
23. Oommen LP, Narayanappa KG (2021) Assimilative capacity approach for air pollution control in automotive engines through magnetic field-assisted combustion of hydrocarbons. *Environ Sci Pollut Res*. <https://doi.org/10.1007/s11356-020-11923-5>
24. Morcos AC, et al (2002) Nd-Fe-B magnets for electric power steering, *EPS Intermag*, pp 3–5
25. Oommen LP, Kumar GN (2022) Experimental analysis of conjoint effect of semi-cooled exhaust recirculation in magnetic field assisted combustion of liquid phase hydrocarbons. *Arab J Sci Eng*. <https://doi.org/10.1007/s13369-022-06842-1>